

# Exoplanet search with astrometry

R. Launhardt

*Max Planck Institute for Astronomy, Königstuhl 17, 69117 Heidelberg, Germany*

---

## Abstract

Searching for extrasolar planets by direct detection is extremely challenging for current instrumentation. Indirect methods, that measure the effect of a planet on its host star, are much more promising and have indeed led to the discovery of nearly all extrasolar systems known today. While the most successful method thus far is the radial velocity technique, new interferometric instruments like PRIMA at the VLTI will enable us to carry out astrometric measurements accurate enough to detect extrasolar planets and to determine all orbital parameters, including their orbit inclination and true mass. In this article I describe the narrow-angle astrometry technique, how it will be realized with PRIMA, what kind of planets we can find, and what kind of preparatory observations are required.

*Key words:*

Techniques: interferometric, astrometry, planetary systems

---

## 1. Introduction

The discovery of planets orbiting stars other than our Sun is one of the greatest scientific and philosophical achievements of our time. Aside from providing us with a wealth of information to understand the formation and structure of planetary systems in a universal context, it captures the interest of both scientists and the public with the prospect of finding life in the Universe. Triggered by the discovery of the first planet orbiting another solar-like star in 1995 [24], more than 300 extrasolar planets have been discovered, the majority of them by using the radial velocity method. The dominant role of this technique is however being eroded by the arrival of new facilities.

The European Southern Observatory (ESO) is currently integrating and testing PRIMA, the instrument for **Phase-Referenced Imaging and Micro-arcsecond Astrometry** [6, 7, 8, 9] at the Very Large Telescope Interferometer on Cerro

Paranal in Chile. The VLTI consists of four stationary 8.2-m VLT "Unit Telescopes" (UTs), four movable 1.8-m "Auxiliary Telescopes" (ATs), and six long-stroke delay lines (DLs). It provides baselines of up to 200 m and covers a wavelength range that extends from the near infrared ( $1\ \mu\text{m}$ ) to  $13\ \mu\text{m}$  [37, 38].

PRIMA will implement the dual-feed capability at the VLTI, at first for two UTs or ATs, to enable simultaneous interferometric observations of two objects that are separated by up to 1 arcmin. PRIMA consists of

1. Star Separators (STS) for each telescope (at first two) that separate two sub-fields (with a star in each) from the telescope field-of-view and send them as collimated beams through the interferometer,
2. Differential Delay Lines (DDLs) that compensate for the optical path difference (OPD) between the two stars,
3. Fringe Sensor Units (FSUs), which combine the beams and detect the interferometric fringes, and
4. an end-to-end laser metrology system (PRIMET) that measures the OPDs within the interferometer.

PRIMA is designed to perform narrow-angle astrometry in K-band with two ATs as well as external fringe-tracking for phase-referenced aperture synthesis imaging with UTs or ATs and instruments like AMBER [31] and MIDI [21].

The PRIMA facility will soon provide us with the infrastructure to carry out an astrometric search for extrasolar planets. This will both complement some weaknesses inherent to the radial velocity method as well as open new discovery spaces. In order to speed up the full implementation of the astrometric capability and to carry out a large astrometric planet search program, a consortium lead by the Observatoire de Genève (Switzerland), Max Planck Institute for Astronomy, and Landessternwarte Heidelberg (Germany), has built Differential Delay Lines (DDLs) for PRIMA [29] and is currently developing the astrometric observation preparation and data reduction software [11]. When PRIMA becomes fully operational in 2010, the consortium will use it with two ATs to carry out a systematic astrometric Exoplanet Search with PRIMA (ESPRI) [16, 17, 18, 19, 20, 34, 35].

## 2. Extrasolar planets - overview on search methods

There are various methods to detect planets around other stars [30]. One can distinguish two detection principles:

1. **Direct methods** detect photons (or other signals) that come directly from the planet.

2. **Indirect methods** measure the influence of a planet on its host star. The presence of a planet is deduced via models.

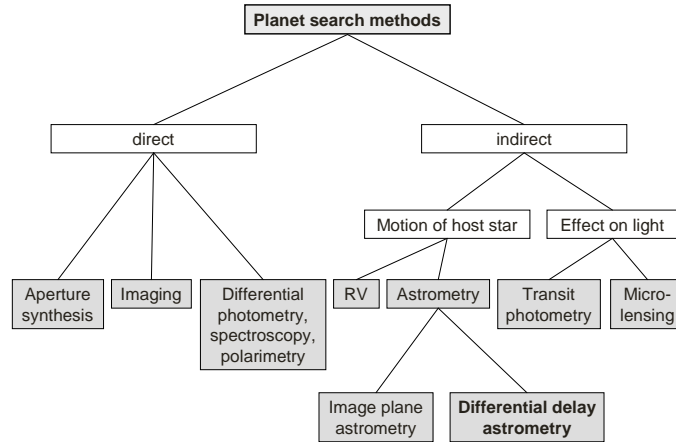


Figure 1: Schematic overview of the most widely used planet search methods

Direct imaging has to overcome the problems caused by the huge brightness contrast (between  $10^6 : 1$  and  $10^9 : 1$ , depending on planet, star, and wavelength) and the small angular separation between star and planet (1 AU at 10 pc distance corresponds to  $0.1''$  projected separation). Therefore, even the most advanced current-day and near-future telescopes and cameras can detect only exceptionally bright planets in large orbits around nearby stars with low mass and luminosity. Other direct methods that include differential imaging and spectroscopy, possibly combined with polarimetry, are now sufficiently advanced to lead to detections of certain planetary systems [15, 23]. Aperture synthesis imaging with interferometers, that could include nulling of the star light, may eventually become a method to directly detect Earth-like planets. But, this technology is not yet advanced enough.

At present, indirect methods are better-suited and more widely used to search for extrasolar planets. The two principle indirect methods measure *(i)* the effect of the planet on the star light, and *(ii)* the effect on the motion of the host star (see Fig. 1). Methods that measure the effect on the light from the star star include:

- **Transit photometry**, which measures the dimming of the light when a planet moves in front of its host star. This method is sensitive only to planetary systems that have their orbital planes aligned with the line of sight towards the Earth [4].
- **Microlensing**, which measures the apparent magnification of the light from a background star due to relativistic light-bending when a planet moves in the line of sight between a distant background star and the Earth [1].

Since the gravitational influence of a planet on its host star is well-defined by Kepler's laws, planet searches today mostly measure the motion of a star as it orbits around the barycenter of the star–planet system. Due to the large mass ratio between star and planet ( $\approx 1,000 : 1$  for Sun and Jupiter and  $\approx 330,000 : 1$  for Sun and Earth), the common center of mass is usually located very close to the star (the center of mass between Sun and Jupiter is located approximately on the surface of the Sun). Consequently, the wobble of the star is quite small and not easy to measure. Although we cannot directly measure the three-dimensional motion of a star on the sky, there are two alternative approaches of measuring different components of this motion:

- The **Radial Velocity (RV) technique** determines the velocity component of the star's motion along the line of sight by measuring the Doppler shift of narrow spectral lines [5]. It measures only one of the three space components of the star's motion and, therefore, leaves the inclination of the orbit undetermined and provides only a lower limit on the mass of the planet. Nevertheless, it is thus far the most successful technique that has led to the discovery of most of the more than 300 known extrasolar planets [36].
- The **astrometric technique** measures the change of the projected position of a star in the plane of the sky (see Fig. 2). The amplitude of this positional "wobble" is very small and not easy to measure. For example, Jupiter causes the Sun to move by  $\approx 1$  mas over 12 yrs when viewed from a distance of 10 pc. Since the astrometric method measures two components of the star's motion (x and y in the plane of the sky), it has the potential of determining all orbital parameters and the true mass of the planet. While astrometry on images is limited by the aperture size and optical properties (distortions) of the telescopes used, astrometric measurements with an interferometer have the potential to reach a much higher accuracy [33].

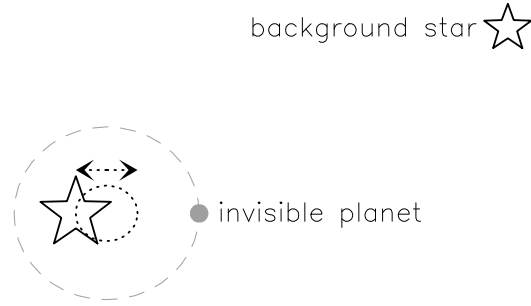


Figure 2: Detecting a planet via astrometric measurements of the host star’s position. Both planet and star orbit around their barycenter, which is, due to the large mass ratio between the two, usually located very close to the star. While the planet itself remains invisible, the “wobble” of its host star in the plane of the sky can be measured directly. A background star serves as position reference.

### 3. Astrometry with an interferometer

#### 3.1. Wide-angle astrometry

A single-star interferometer measures the delay,  $d$ , (or OPD) between the sections of the wavefront from a star as they arrive at the two telescopes [12, 13]. This delay is given by:

$$d = \vec{s} \cdot \vec{B} + C = B \cdot \cos \theta + C \quad , \quad (1)$$

where  $\vec{s}$  is the direction vector to the star,  $\vec{B}$  is the baseline vector (and  $B$  its length),  $\theta$  is the angle between  $\vec{s}$  and  $\vec{B}$ , and  $C$  is a fixed instrumental term that must be calibrated (see Fig. 3).  $\theta$  corresponds to the position angle of the star on the sky, projected onto the baseline. The external delay, which cannot be measured directly, is compensated with an optical delay line (DL) in the interferometer. At the position of the maximum stellar fringe, external and internal delays are equal. An approximation to the internal delay is measured with a laser metrology system. Thus, by precisely knowing the interferometer baseline and measuring the delay, one can determine the position angle of the star with respect to the baseline with a precision that is no longer limited by the aperture size of the telescopes. Atmospheric perturbations, however, introduce random piston fluctuations which add up to the the measured total delay. Although this could be partially overcome by observing at two wavelengths, it limits the astrometric accuracy to the mas level.

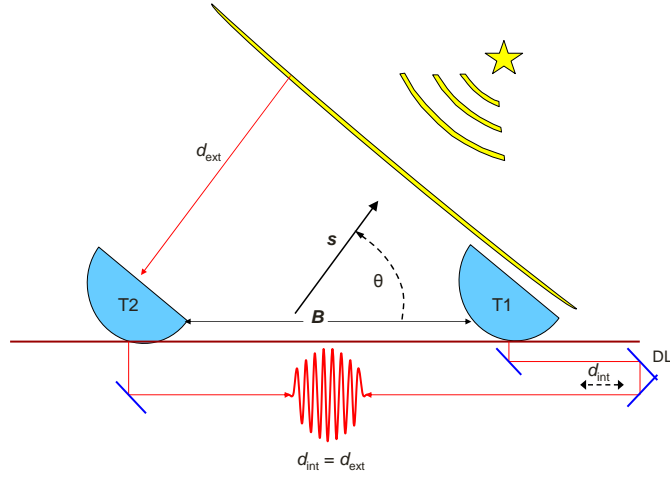


Figure 3: Single-star astrometry with an interferometer.

### 3.2. Narrow-angle astrometry

To circumvent this problem, a dual-star interferometer like PRIMA measures only the differential delay between two stars, which corresponds to the angular separation between the two stars on the sky, projected onto the baseline. If the angular separation between the two stars is smaller than the isopiston angle of the atmosphere, where the piston perturbations and hence the fringe motions of the two wavefronts are correlated, the mean differential piston perturbations average to zero for sufficiently long observing time [39]. The differential delay,  $\Delta d$ , is then given by:

$$\Delta d = \Delta \vec{s} \cdot \vec{B} + \Delta C = \Delta s \cdot B \cdot \cos \phi + \Delta C \quad , \quad (2)$$

where  $\Delta \vec{s}$  is the separation vector between the two stars in the plane of the sky,  $\phi = 90^\circ - \theta$  is the angle between the separation vector and the baseline vector, and  $\theta$  is the angle between the the baseline vector and the direction towards projected central position between the two stars (see Fig. 4). The differential instrumental delay,  $\Delta C$ , is close to zero and can be calibrated. In contrast to  $\vec{s}$ ,  $\Delta \vec{s}$  is no longer a unit vector.

The calibrated differential delay (Eq. 2) is then proportional to the projection of the separation vector between the two stars onto the interferometer baseline, i.e., it is a one-dimensional measurement. In order to obtain both dimensions of the separation vector, one has to observe either with two different (orthogonal) baselines, or with one baseline at different parallactic angles.

This dual-star technique has another advantage besides providing a reference against which positional offsets can be measured (narrow-angle astrometry). If one of the two stars (the “primary star”) is bright enough to measure its fringe phase within the atmospheric coherence time (fringe-tracking), it can be used to stabilize the fringes on the other (secondary) star (phase-referencing), thus allowing for much longer coherent integrations and hence increasing the limiting magnitude and the number of observable objects.

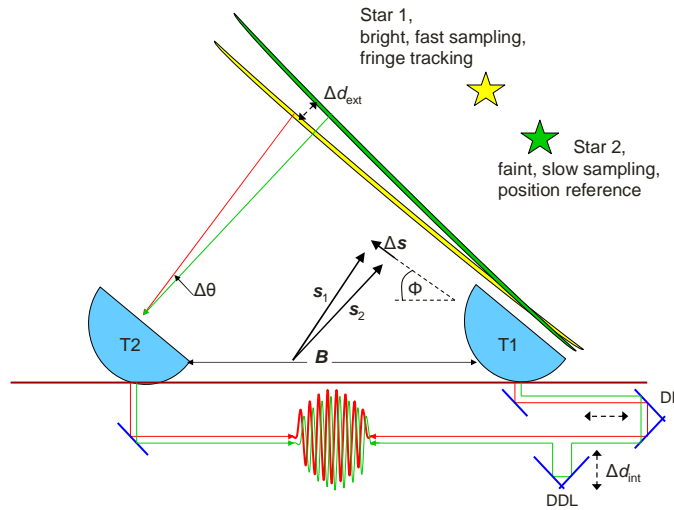


Figure 4: Narrow-angle astrometry with a dual-star interferometer.

### 3.3. Astrometry with PRIMA

PRIMA will be the third optical / IR long-baseline dual-star interferometer that can perform narrow-angle astrometry as described above (see Sect. 3.4). In its astrometry mode, PRIMA will mainly work with the 1.8 m ATs, because they have much less severe vibration problems than the UTs. Phase-referenced imaging does not depend so much on the highest possible OPD accuracy and will, therefore, preferably be done with the larger UTs.

In PRIMA, Star Separator units (STS) located at the Coudé focus of each telescope separate two sub-fields (with a star in each) from the telescope field-of-view and send them as collimated beams through the interferometers. The two beams from each telescope are first sent parallel and close to each other through one main delay line (DL), to compensate the large delay that is common to both stars. This

ensures that differential perturbations between the two beams introduced in the long DL tunnels are kept at a minimum. To obtain fringes from both stars on the detector, the differential OPD (dOPD) between the two stars must also be compensated. This is done with four Differential Delay Lines (DDLs; see Fig. 4), one for each star and telescope. Although the measurement principle would require only one DDL, operational reasons and symmetry requirements for the interferometer lead to the design with one DDL for each beam. The dOPD for two stars separated by less than an arcmin is much smaller (up to a few cm only) than the main OPD. But, its compensation requires that the two beams travel different path lengths, giving rise to differential longitudinal dispersion (the metrology works at a different wavelength than the observed starlight) and other distortions that affect the dOPD measurements. Therefore, the DDLs operate in vacuum.

After the four beams have traveled through the main DLs and the DDLs, they arrive in the subterranean interferometric laboratory, where the Fringe Sensor Units (FSUs) and the other interferometric instruments are located (currently AMBER and MIDI). The beams from the bright star are combined and the fringe phase (for fringe-tracking) and group delay (for astrometry) measured in one of the two FSUs. This happens at a frequency of about 1 kHz to sample the atmospheric coherence time of  $\approx 1$  ms in K-band. The FSUs combine the beams in the pupil plane, but they do not scan the fringes by modulating the OPD. Instead, the combined beam is split into four output beams that are shifted in phase with respect to each other (relative phases of the four beams:  $0, \pi/2, \pi, 3\pi/2$ ). The intensities of these four beams, from which the phase of the input beam is computed, are then measured by an infrared camera. The offset from zero phase of the bright star is used to control the DLs and DDLs and modify the internal OPD such that the phase is brought back to zero. In astrometry mode, the beams from the other (fainter) star are combined in the same way in the second FSU. Since the OPD corrections, derived from the real-time fringe measurements on the bright star with the first FSU, are also applied to the beams of the faint star, this second FSU can now integrate much longer (several seconds) to detect the fringes without smearing them and measure their position. The total integration time of typically 30 min is built up by continuously repeating this sequence.

A laser metrology system is used to measure the internal dOPD in the interferometer between the two stars. This H-band laser beam is injected into the star beams inside the FSU beam combiners, travels “backwards” through the entire VLTI optical train until it is reflected back at a retroreflector which is located between the STS and the telescope Coudé train with the derotator. This retroreflector, or more precisely, its image in the entrance pupil of the telescope, is the



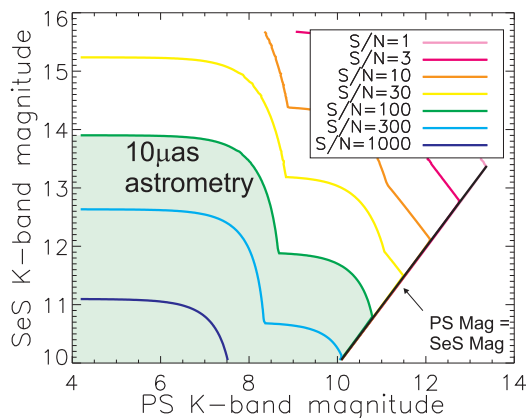


Figure 5: Dependence of astrometric accuracy of PRIMA with two ATs on brightness for  $10''$  separation between primary (PS) and secondary (SeS) star and 30 min integration [40, 20]. Note that this figure is the result of an error budget simulation, based on PRIMA subsystem specifications, but without knowing the actual throughput and performance of all components. These actual sensitivity of PRIMA must be verified on real stars during commissioning in 2009.

reference point for OPD measurements which separate the differential delay  $\Delta d$ , measured by PRIMET, from the baseline,  $\vec{B}$  (Eq. 2).

In order to be able to eliminate the constant term  $\Delta C$  in Eq. 2 from the measurements, it is necessary to periodically exchange the two stars within the instrument during an astrometric measurement. This will be done by turning the field derotators in the AT Coudé trains by  $180^\circ$ . This implies that calibrated delays cannot be derived before the observing sequence is finished.

With two ATs, the minimum K-band brightness of primary stars, required for fringe-tracking is  $K \approx 8$  mag. The astrometric accuracy of PRIMA is directly related to the accuracy of the interferometric differential phase measurement. The S/N of the visibility phase is in turn proportional to the visibility amplitude of the interferometric fringes. A S/N of 100 of the detection of the cross-visibility would correspond to an interferometric differential phase error of  $1/100$  radians. At a wavelength of  $2.2 \mu\text{m}$ , this corresponds to an OPD error of 3.5 nm. On a 150 m baseline (typical for PRIMA astrometry), this corresponds to an astrometric error of  $\approx 5 \mu\text{as}$ . This accounts for about half of the anticipated OPD error of PRIMA, the other half coming mainly from seeing effects. Therefore, a S/N of 100 for the fringe detection of the reference star has been assumed to be necessary for reaching an astrometric accuracy of  $10 \mu\text{as}$ . In 30 min integration time, this can be reached on a  $K \leq 14$  mag star [40, 20] (see Fig. 5). Note that both

the limiting magnitude for fringe-tracking as well as the brightness constraint on reference stars are model estimates, which must be verified on real stars during the commissioning of the instrument in 2009.

The isopistonc angle at Paranal and in K-band is  $\approx 10\text{-}20''$ ; a value that will also be verified during PRIMA commissioning. The optical design of the STS does not allow to separate stars closer than  $2''$  without diverting light into the other channel. Therefore, there is not only a maximum angular separation, limited by the isopistonc angle of the atmosphere, but a minimum as well.

For astrometry with PRIMA, AT baselines with 80 – 160 m length will typically be used. On a 100 m baseline, a separation of  $10''$  between two stars corresponds to an OPD of  $\approx 5$  mm in the interferometer, which must be compensated with the DDLs. The anticipated measurement accuracy of  $10\ \mu\text{as}$  corresponds to a dOPD of only 5 nm. This number defines the total dOPD error budget for PRIMA in the astrometric mode. Since the limitation due to residual atmospheric turbulence during a 30 min integration will be of the same order, we expect to reach a final single astrometric measurement accuracy of  $\approx 15 - 20\ \mu\text{as}$ .

#### *3.4. Narrow-angle astrometry with other instruments*

PRIMA is not the only instrument that can perform narrow-angle astrometry. The first real narrow-angle astrometry measurements were done in 1992 at the Mark III interferometer [3]. The PHASES project [28] at the Palomar Testbed Interferometer (PTI, [2]) has successfully demonstrated  $100\ \mu\text{as}$  differential astrometry and two-combiner phase referencing. It can perform differential astrometry on bright binary stars with separations in the range of 0.1-1.0 arcseconds. The ASTRA upgrade of the Keck Interferometer will enable soon narrow-angle astrometry with an anticipated accuracy of  $\approx 100\ \mu\text{as}$  on star pairs with separations and brightness limits similar to PRIMA [32]. GRAVITY, an interferometric imager for the VLTI with astrometric capability, but with a total field of view of only  $1.7''$ , is currently being developed and will enable  $10\ \mu\text{as}$  very narrow-angle astrometry on galactic center stars after 2012 [10]. The most important upcoming astrometric space missions, Gaia and SIM Lite, will not rely on real narrow-angle (dual star) astrometry, but shall be mentioned here because in particular SIM also addresses similar scientific questions as PRIMA and my thus be relevant to extent the time baseline for certain PRIMA targets.

#### 4. Prospects for planet detections with astrometry

The RV method is very efficient in detecting planets in short-period orbits close to the star. It requires stars with a sufficient number of narrow spectral lines, i.e., fairly old stars (Gyrs) of about  $1.2 M_{\odot}$  or less. More massive stars ( $M > 1.4 M_{\odot}$ ) as well as young and chromospherically active stars are often excluded from RV planet searches because their RV is more difficult to determine. Stars  $M > 1.4 M_{\odot}$  have only very few usable spectral lines. Young and active stars have often broad (rapid rotators) and unstable (chromospheric activity) lines. Correspondingly, our knowledge on the RV planet population is biased towards planets in short and intermediate-period orbits around solar-type stars. RV measurements also provide no constraint on the inclination of the orbit ( $\sin i$ ), and thus usually only a lower limit on the planetary mass can be derived. For this reason, astrometric orbit measurements are ultimately required to derive the fundamental parameter of a planet: its mass. However, to play a significant role and open new discovery spaces, an astrometric accuracy of order  $10\text{--}50 \mu\text{as}$  is needed.

The semi-amplitude of the RV variation,  $K_1$ , follows from Kepler’s laws and is given by

$$K_1 = \frac{m_p \sin i}{(m_* + m_p)^{2/3}} \cdot \sqrt[3]{\frac{2\pi G}{P}} \cdot \frac{1}{\sqrt{1 - e^2}} \quad , \quad (3)$$

where  $m_p$  is the mass of the planet,  $m_*$  is the mass of the star,  $i$  is the inclination angle of the orbital plane against the line of sight,  $P$  is the orbital period,  $G$  is the gravitational constant, and  $e$  is the orbital eccentricity.

Astrometry, on the other hand, is a complementary technique with a different detection bias. It favors planets in wide, long-period orbits (like in our own Solar System). Furthermore, astrometry can measure two components of the stellar reflex motion, versus the single radial component that is observable spectroscopically, thus allowing to derive full orbit solutions. From the definition of the barycenter of a two-body system, one can easily derive the semi-amplitude of the astrometric “wobble” of a star that is orbited by a planet:

$$\rho = \frac{m_p}{m_* + m_p} \cdot \frac{a}{D} \quad , \quad (4)$$

where  $a$  is the distance between the two bodies’ centers and  $D$  is the distance towards the objects. Invoking Kepler’s third law and neglecting eccentricity (i.e., assuming  $e = 1$ ), gives:

$$\rho = \frac{m_p (m_* + m_p)^{1/3}}{m_*} \cdot \sqrt[3]{\frac{P^2 G}{4\pi^2}} \frac{1}{D} \quad . \quad (5)$$

Equations 3 and 5 show the different detection biases of the two methods: RV ( $K \propto P^{-1/3}$ ) is more sensitive to planets in short-period orbits, while astrometry ( $\rho \propto P^{+2/3}/D$ ) favors planets in longer-period orbits. This is also demonstrated in Fig. 6, which shows the detection limits for planet searches with astrometry and the radial velocity technique in a planet mass vs. orbital period diagram. To illustrate which method is sensitive to what kind of planets, the detection curves are overplotted on a planet population synthesis for solar mass stars, based on the core accretion paradigm [27] as well as the already known extrasolar planets. The diagram shows that narrow-angle astrometry with an accuracy of  $50 \mu\text{as}$  ( $5 \sigma$ ) opens a new discovery space only for orbital periods longer than 1–3 yrs. Although the exact location of the crossing point between the two detection curves depends on the characteristics of the specific target stars (e.g., distance, mass, activity levels) and may shift over time (better spectrographs), this estimate has important implications for target selection and observing strategies of astrometric planet search programs.

When equipped with Differential Delay Lines, PRIMA will be able to perform narrow-angle astrometry in K-band with a single-measurement accuracy of up to  $10\text{--}20 \mu\text{as}$ . Although this ultimate accuracy goal may only be reached after at least 1 yr of data will have been used for long-term calibrations (see Sect. 5), it will be capable of detecting Saturn-mass planets around nearby main sequence stars of any spectral type, down to Uranus-mass planets in 1–5 AU orbits around nearby M dwarfs. This peak of the ice giant distribution is outside the reach of current-day RV measurements. Since astrometry does not depend on narrow and stable spectral lines, it will also be sensitive to Jupiter-like giant planets around young stars which are less suitable for the RV method. Earth-like rocky planets are, however, still out of reach for current-day ground-based astrometry.

## 5. The ESPRI project: astrometric exoplanet search with PRIMA

Starting in 2010, when PRIMA will be commissioned and operational, the ESPRI consortium (see Sect. 1) will use the facility with two ATs to carry out an astrometric Exoplanet Search program with PRIMA (“ESPRI”). ESPRI will address the following outstanding issues:

- Resolve the *sin i* uncertainty from planet masses found by RV surveys and derive accurate planet masses. This measurement is fundamental to study the planetary mass function, in particular the upper mass cut-off where the statistics is poor.

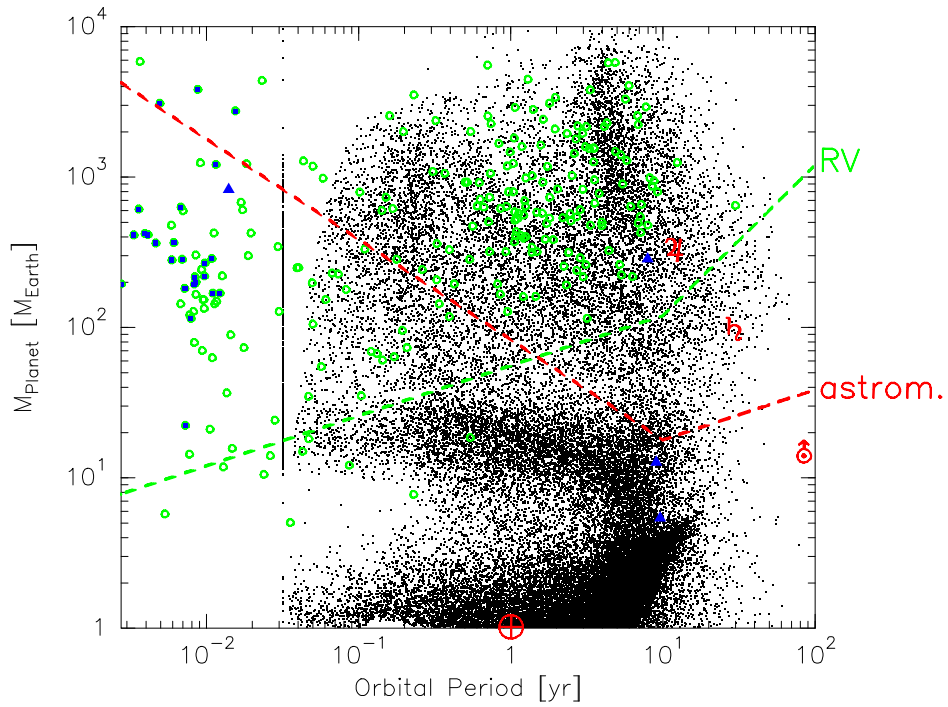


Figure 6: Detection spaces (planet mass vs. orbital period) for planet searches with astrometry and the RV technique. Black dots represent the results of a planet population synthesis for solar mass stars, based on the core accretion paradigm [27]. Inward migration was artificially stopped at 0.1 AU, which explains the pile-up line at 0.03 yrs and the discrepancy between model and observations for hot Jupiters. Known extrasolar planets are marked as green circles (RV, lower mass limit due to *sin i* uncertainty), blue squares (transit photometry), and blue triangles (microlensing). Solar system planets are marked in red by their respective symbols. Detection thresholds are marked by dashed lines under the following assumptions: host star mass  $1 M_{\odot}$ , RV detection limit 5 m/s, astrometric detection limits  $50 \mu\text{as}$  at distance 5 pc, maximum timeline of observations 10 yrs. Note that many of the known RV planets are detected around stars with masses lower than  $1 M_{\odot}$  and therefore can appear below the RV detection threshold for  $1 M_{\odot}$  stars.

- Confirmation of hints for long-period planets in RV surveys.
- Measure the relative orbit inclinations in multiple planetary systems.
- Inventory of planets around stars with different mass and age. Of particular interest are the most nearby stars, irrespective of their spectral type, as well as young stars with ages up to few hundred Myr.

Table 1: Pre-selected ESPRI target stars

|                                 | RV:                     | CNS:                    | YS:                   |
|---------------------------------|-------------------------|-------------------------|-----------------------|
| Brightness <sup>1)</sup> :      | $K \leq 8$ mag          | $K \leq 8$ mag          | $K \leq 8$ mag        |
| Distance:                       | $D \leq 200$ pc         | $D \leq 15$ pc          | $D \leq 100$ pc       |
| Age:                            | no restriction          | no restriction          | $a \leq 300$ Myr      |
| Spectral types:                 | F7 ... M3 <sup>2)</sup> | A3...M6.5 <sup>2)</sup> | B8...M3 <sup>2)</sup> |
| Selection sources:              | www.exoplanet.eu        | CNS <sup>3)</sup>       | [22, 26, 41]          |
| Number of stars <sup>4)</sup> : | 148                     | 367                     | 380                   |

<sup>1)</sup> Derived from the expected limit for hardware fringe-tracking. Astrometry with reduced accuracy might be possible also on fainter stars (see Fig. 5).

<sup>2)</sup> No a priori restriction, but the limitations in brightness and distance constrain the spectral types of the available stars. For group RV we also include sub-giants (luminosity class IV).

<sup>3)</sup> Unpublished version of the Catalogue of Nearby Stars [14] from August 2005 (Jahreiss, priv. comm.).

<sup>4)</sup> Known spectroscopic binaries and visual binaries with projected separation  $< 2''$  are already excluded.

With these scientific goals in mind, three lists with potential target stars were preselected for the ESPRI project (see Table 1):

1. **RV:** Stars with known RV planets within  $\leq 200$  pc around the Sun.
2. **CNS:** Nearby stars of any spectral type within  $\leq 15$  pc around the Sun.
3. **YS:** Young stars with ages  $< 300$  Myr within  $\leq 100$  pc around the Sun.

This preselected list contains in total about 900 stars. Of course, only stars that have suitable reference stars within the isopistonc angle can be observed with PRIMA. If such reference stars are available or not must be determined for every single star of this input list (see Sect. 6). With the constraints on separation

( $2'' - \approx 20''$ ) and brightness ( $K \leq 14$  mag for SNR 100 in 30 min integration time; see Sect. 3.3 and Fig. 5), one can expect to find on average one good target out of 10 candidates (10%). Of course, the detection rate depends strongly on Galactic latitude, so the final ESPRI target list will be heavily biased towards the Galactic plane. In total, the ESPRI project will monitor about 100 stars during about 200 nights spread over 5 years from 2010 through 2015.

## 6. Necessary preparatory observations

Both narrow-angle astrometry as well as phase-referenced imaging of faint objects rely on the availability of reference stars within the isopistonc angle around the target object. For faint source imaging this can be a real obstacle since the reference star must be bright enough for fringe-tracking. It is usually very unlikely to find such a bright star so nearby a pre-selected faint target object.

The situation is somewhat more favorable for narrow-angle astrometry of stars that are bright enough for fringe-tracking. Although it strongly depends on the Galactic latitude, it is much more likely to find a fainter background star nearby any given foreground star than vice versa. In this case, however, other problems become evident.

Most public data bases are either not sensitive enough and therefore miss most of the potential reference stars, or they suffer from strong saturation and “blind” areas around bright stars ( $K < 8$  mag or  $V < 3 \dots 7$  mag) (e.g., 2MASS, Denis, DSS2, SDSS; see Fig. 7). Others, like USNO B1.0 [25], are so much dominated by ghosts and artefacts around bright stars that the false alarm rate is close to 100%, while actually existing stars remain undetected. For these reasons it turns out that existing public data bases cannot be used to reliably identify reference stars for PRIMA observations. Therefore, dedicated preparatory observations are a key pre-requisite for any PRIMA observation.

Ideally, one would wish to use adaptive optics together with a coronagraphic near-infrared camera to hunt for faint background stars very close to very bright foreground stars. However, such instruments are usually not available and would be “too expensive” for preparatory observations only. With dedicated “standard” NIR photometric imaging observations, optimized for high dynamic range, the problems of saturation effects and ghost images can be minimized (but not completely avoided) when the following advice is taken into account. The total integration time should be built up by using the shortest possible single detector integration time (DIT), which is usually 1–2 sec for many NIR cameras. This requires a camera with very fast readout scheme; otherwise the readout overhead

will quickly exceed the on-source integration time. Even then, the target stars will usually saturate, but it should now be possible to identify faint background stars as close as 1-3'' to the bright star (see Fig. 7).

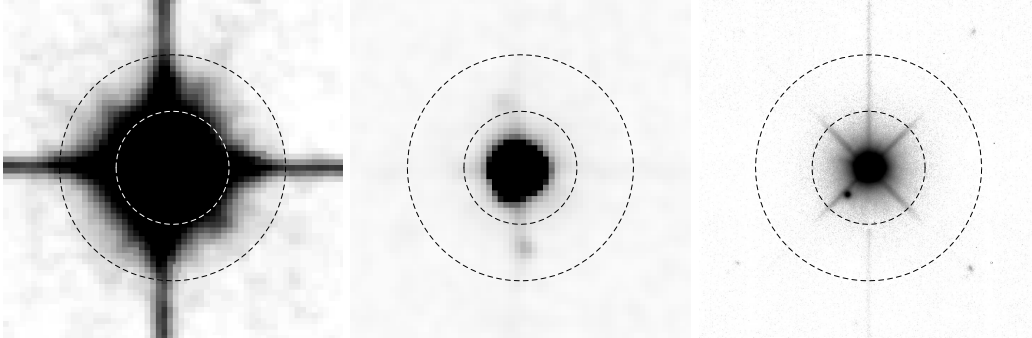


Figure 7: Three images of HD 87978, a potential ESPRI target star. Left: DSS2-red, Center: 2MASS-K, Right: our high dynamic range K-band image obtained with SOFI at the ESO NTT in March 2008. North is up and East is left. The two circles denote radii of 10'' and 20'' around the target star. The star itself has  $K \approx 6.5$  mag. The potential reference star at  $r \approx 6''$  separation from the target has  $K \approx 12$  mag. Objects such close to a very bright star are usually not detected in 2MASS, DSS, or other all-sky surveys.

An instrument that is currently (still) available at ESO and is suited to perform such a search for PRIMA reference stars is SOFI at the NTT at the La Silla observatory. Figure 7 shows what can be done with SOFI when the above-mentioned rules are followed, as compared to all-sky surveys like DSS or 2MASS.

While the search for reference stars is a mandatory task when preparing any PRIMA observations, spectroscopic observations might be useful to characterize the target stars and to identify excessively active stars and spectroscopic binaries. The first ones could produce a too large astrometric “noise”. Spectroscopic binaries are both in terms of fringe detection and interpretation and planet formation and orbit stability not well-suited to perform an astrometric planet search.

## 7. Summary

This article gives an overview on how ground-based astrometric observations with an interferometer can be used to search for extrasolar planets. A facility that will soon become operational and is accessible to the ESO community is PRIMA.



Sect. 2 gives a general overview on planet search methods and, in particular, compares the two indirect methods RV technique and astrometry.

Sect. 3 explains how astrometric measurements are done with an interferometer, and how this is technically realized in PRIMA. The key points are: *(i)* a dual-beam interferometer is needed to simultaneously observe two stars that are located within the same isopiston patch of the atmosphere, *(ii)* the interferometer measures the differential delay between the wavefronts from the two stars, and *(iii)* the differential delay and the interferometer baseline are directly related to the part of the angular separation vector between the two stars that is projected onto the baseline. In order to reach the anticipated astrometric accuracy of 10-20  $\mu\text{as}$ , PRIMET metrology can measure the dOPD in the interferometer with an accuracy of 5 nm. The (narrow-angle) baseline will be determined with an accuracy of  $\approx 50 \mu\text{m}$ . With two ATs, the minimum K-band brightness of primary stars, required for fringe-tracking, is  $K \approx 8$  mag. The minimum K-band brightness of reference stars required to reach 10  $\mu\text{as}$  in about 30 min integration time is  $K \leq 14$  mag. The angular separation between the two stars must be  $2'' < \Delta s < \approx 20''$ .

Sect. 4 outlines the exoplanet detection space of a 10  $\mu\text{as}$  astrometric facility and compares it to the RV detection space. Both methods have opposite detection biases with respect to the orbital period, with astrometry being more sensitive to longer period planets. In particular, narrow-angle astrometry with an accuracy of 50  $\mu\text{as}$  ( $5\sigma$ ) opens a new discovery space only for orbital periods longer than 1–3 yrs and can detect Uranus-mass planets in 1–5 AU orbits around nearby M dwarfs. Earth-like rocky planets are, however, still out of reach for current-day ground-based astrometry.

Sect. 5 gives an overview on the astrometric planet search project that the ESPRI consortium wants to carry out with PRIMA between 2010 and 2015. Particular targets of the ESPRI programme are: *(i)* Stars with known exoplanets detected by RV, *(ii)* the most nearby stars ( $D \leq 15$  pc) around the Sun, and *(iii)* nearby young stars with  $D \leq 100$  pc around the Sun.

Sect. 6 describes which preparatory observations are necessary before a star can be astrometrically observed with PRIMA. In particular it is mandatory to search for reference stars around the potential target stars. Since available all-sky surveys often miss faint background stars close to very bright foreground stars (the typical planet search targets), dedicated high dynamic range NIR imaging observations are often unavoidable.

## References

- [1] Bennett, D. P., & Rhie, S. H. 2002, *ApJ*, 574, 985
- [2] Boden, A. F. 2004, *Proc. SPIE*, 5491, 506
- [3] Colavita, M. M. 1994, *A&A*, 283, 1027
- [4] Charbonneau, D., Brown, T. M., Burrows, A., & Laughlin, G. 2007, *Proto-stars and Planets V*, 701
- [5] Cumming, A., Marcy, G. W., & Butler, R. P. 1999, *ApJ*, 526, 890
- [6] Delplancke, F., Leveque, S. A., Kervella, P., Glindemann, A., & D'Arcio, L. 2000, *Proc. SPIE*, 4006, 365
- [7] Delplancke, F., et al. 2006, *Proc. SPIE*, 6268
- [8] Delplancke, F. 2008, *New Astronomy Review*, 52, 199
- [9] Derie, F., Delplancke, F., Glindemann, A., Lévêque, S., Ménardi, S., Paresce, F., Wilhelm, R., & Wirenstrand, K. 2003, *GENIE - DARWIN Workshop - Hunting for Planets*, 522
- [10] Eisenhauer, F., et al. 2008, *IAU Symposium*, 248, 100
- [11] Elias, N. M., et al. 2008, *IAU Symposium*, 249, 119
- [12] Haniff, C. 2007, *New Astronomy Review*, 51, 565
- [13] Haniff, C. 2009, *New Astronomy Review*, this volume
- [14] Jahreiss, H., & Gliese, W. 1993, in: *Developments in Astrometry and their Impact on Astrophysics and Geodynamics*, *Proc. IAU Symp.* 156, 107
- [15] Kalas, P., et al. 2008, *Science*, 322, 1345
- [16] Launhardt, R., et al. 2005, *Astrometry in the Age of the Next Generation of Large Telescopes*, 338, 167
- [17] Launhardt, R., Henning, T., Queloz, D., & Quirrenbach, A. 2007, *Exploring the Cosmic Frontier: Astrophysical Instruments for the 21st Century*, 265

- [18] Launhardt, R., et al. 2008a, The Power of Optical/IR Interferometry: Recent Scientific Results and 2nd Generation Instruments, 551
- [19] Launhardt, R., et al. 2008b, Proc. SPIE, 7013, 70132
- [20] Launhardt, R., et al. 2008, IAU Symposium, 248, 417
- [21] Leinert, C., et al. 2003, Ap&SS, 286, 73
- [22] Mamajek, E. E., Meyer, M. R., & Liebert, J. 2002, AJ, 124, 1670
- [23] Marois, C., Macintosh, B., Barman, T., Zuckerman, B., Song, I., Patience, J., Lafreniere, D., & Doyon, R. 2008, arXiv:0811.2606
- [24] Mayor, M., & Queloz, D. 1995, Nature, 378, 355
- [25] Monet, D. G., et al. 2003, AJ, 125, 984
- [26] Montes, D., López-Santiago, J., Gálvez, M. C., Fernández-Figueroa, M. J., De Castro, E., & Cornide, M. 2001, MNRAS, 328, 45
- [27] Mordasini, C., Alibert, Y., Benz, W., & Naef, D. 2008, Astronomical Society of the Pacific Conference Series, 398, 235
- [28] Muterspaugh, M. W., Lane, B. F., Konacki, M., Burke, B. F., Colavita, M. M., Kulkarni, S. R., & Shao, M. 2005, AJ, 130, 2866
- [29] Pepe, F., et al. 2008, Proc. SPIE, 7013,
- [30] Perryman, M. A. C. 2000, Reports on Progress in Physics, 63, 1209
- [31] Petrov, R. G., et al. 2000, Proc. SPIE, 4006, 68
- [32] Pott, J.-U., et al. 2009, New Astronomy Review, this volume (arXiv:0811.2264)
- [33] Quirrenbach, A. 2001, ARA&A, 39, 353
- [34] Quirrenbach, A., et al. 2004, Proc. SPIE, 5491, 424
- [35] Reffert, S., et al. 2006, Proc. SPIE, 6268, 424
- [36] Schneider, J. 1995, The Extrasolar Planets Encyclopaedia: <http://exoplanet.eu/>

- [37] Schöller, M. 2007, *New Astronomy Review*, 51, 628
- [38] Schöller, M. 2009, *New Astronomy Review*, this volume
- [39] Shao, M., & Colavita, M. M. 1992, *A&A*, 262, 353
- [40] Tubbs, R. N., Launhardt, R., Meisner, J., et al. 2008, "ESPRI - Exoplanet Search with PRIMA - Astrometric Error Budget", VLT-TRE-AOS-15753-0001, V2.1
- [41] Wichmann, R., Schmitt, J. H. M. M., & Hubrig, S. 2003, *A&A*, 399, 983